J Indian Inst. Sci., May–June 1988, **68**, 223–233
Indian Institute of Science

IISc. THESES ABSTRACTS

Thesis Abstract (Ph.D.)

Classical relativistic particles with internal structure: A group theoretic and differential geometric analysis by Madhusudan V Atre

Research supervisors: S. Krishan and N Mukunda.
Department: Physics.

1. Introduction

This thesis presents a systematic study of internal structures possible for a classical relativistic indecomposable particle without spatial extension Group theoretic and differential geometric methods are used and the Lagrangian formalism of dynamics adopted Based on the assumed indecomposability, the internal spaces Q are kinematically classified in terms of the coset spaces of the group SL(2,C) with respect to its distinct closed continuous subgroups The allowed spaces Q are separated into First Order Spaces, FOS's (of which there are two), and Second Order Spaces, SOS's (of which there are ten distinct ones and two one parameter families). The former Q's admit an SL (2,C) invariant symplectic structure while the latter do not. A search is then made for those cases in which Lagrangians can be constructed involving nontrivial coupling between the space-time coordinates and the internal variables. The resulting Lagrangians describe Regge trajectories, *i.e.* a family of particles characterised by a mass-spin relationship, in the classical limit.

2. Physical principles

The physical principles underlying the study are indecomposability, Poincaré symmetry, and reparametrization invariance of the action. The last mentioned leads, in the canonical formalism, to a primary constraint on the phase space variables which under suitable conditions is the mass-spin relationship The separation of the Q's into FOS's and SOS's is carried out. The forms of the most general Lagrangians, in both the cases, are then described in terms of a maximal set of independent Lorentz scalars constructed out of the space-time and internal variables

3. FOS's, topologies and constrained dynamics

FOS's are related to orbits in the Lie algebra of SL(2,C). Their topological structure and properties are analysed and a Lagrangian description for particles with such internal spaces is shown to exist in both the cases The similarities and differences in the description of the (constrained) Hamiltonian dynamics and the space-time trajectories for the two cases are highlighted. An interesting feature distinguishing them is brought out by means of a calculation of the magnetic moment for particles lying on the Regge trajectory.

4. SOS's, isotopy representations, Lagrangians and phase-space formalism

The SOS's are separated into those which admit a manifestly covariant description and those which do not The former are easily seen to allow a Lagrangian description of dynamics with nontrivial coupling between the space-time and internal variables. The latter are analysed using the concept and methods of the isotopy representation which are set up in detail. It is shown that in three cases it is impossible to couple the internal and the space-time variables in a physically interesting way. Our study reveals that two other cases can be partly, but not completely, described in a manifestly covariant way. An example of the manifestly covariant spaces is worked out displaying the structure of the Lagrangian.

5. Geometric framework

We present a coordinate independent differential geometric description of the work of the previous chapters This is done to provide a different way of looking at the various concepts and to develop a global point of view.

6. Conclusions

The various models existing in the literature are discussed and related to the general classification scheme presented in the thesis. Some interesting problems worth pursuing in the field are also pointed out.

In Appendix A the closed continuous subgroups of SL(2,C) (up to conjugation) are enumerated. In Appendix B, we give a simple-minded proof using local coordinates, of an important theorem of Kostant-Kirillov-Souriau which has been used to study the FOS's. Some results in the geometry of Lie groups and Lie algebras, are given in Appendix C.

References

1. Hanson, A J and Regge, T.	The relativistic spherical top, *Ann. Phys.*, 1974, **87**, 498–566
2. Mukunda, N., Vandam, H and Biededharn, L C	Relativistic models of extended hadrons obeying a mass-spin trajectory constraint, *Lecture notes in physics*, Vol. 165, Springer-Verlag, 1982
3. Atre, M. V and Mukunda, N.	Classical particles with internal structure: General formalism and application to first-order internal spaces, *J. Math Phys*, 1986, **27**, 2908–2919.
4 Atre, M V. and Mukunda, N.	Classical particles with internal structure II: Second-order internal spaces, *J Math Phys.*, 1987, **28**, 792–806.
5. Atre, M V	Geometry of classical particles with internal structure, 1987, TIFR/TH/87–9

Photochemical and X-ray crystallographic studies on coumarins in the crystalline state by K. Gnanaguru.

Research supervisor: V. Ramamurthy.
Department: Organic Chemistry.

1. Introduction

The thesis deals with the photochemical studies of 16 substituted coumarins (fig. 1) with substituents such as chloro, acetoxy, methyl, methoxy and hydroxyl and the X-ray crystallographic analyses of four coumarins. It has been reported earlier that the crystals of coumarin do not

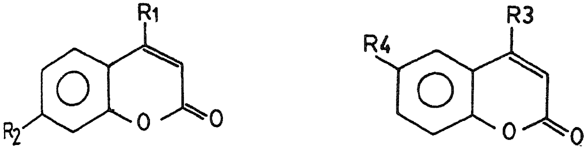

1 $R_1 = H$, $R_2 = Cl$; 2. $R_1 = H$, $R_2 = Me$; 3. $R_1 = Me$, $R_2 = Cl$; 4. $R_1 = Me$, $R_2 = OAc$; 5. $R_1 = OAc$, $R_2 = H$; 6. $R_1 = Me$, $R_2 = H$.

7. $R_3 = H$, $R_4 = Cl$; 8. $R_3 = H$, $R_4 = Me$; 9. $R_3 = H$, $R_4 = OH$; 10. $R_3 = H$, $R_4 = OMe$; 11. $R_3 = H$, $R_4 = OAc$; 12. $R_3 = Me$, $R_4 = Cl$; 13 $R_3 = Me$, $R_4 = Me$; 14. $R_3 = Me$, $R_4 = OH$; 15. $R_3 = Me$, $R_4 = OMe$; 16. $R_3 = Me$, $R_4 = OAc$.

FIG. 1 Coumarins investigated.

undergo photodimerization owing to the unfavourable molecular packing in the crystal lattice[1]. Thus it provided a simple molecular framework for investigating the role of substituents on molecular packing conducive for photoreactivity.

Of the 16 coumarins studied, the crystals of 6-chloro, 7-chloro, 4-methyl-6-chloro, 4-methyl-7-chloro, 6-acetoxy, 4-methyl-7-acetoxy, 6-methoxy and 7-methyl coumarins were found to be photoreactive. The photodimerization of these eight coumarins was monitored by IR and ^{1}H-NMR spectroscopic analysis The yield of dimer was determined by NMR integration. The dimerization of 6-methoxy, 4-methyl-6-chloro and 7-methyl coumarins exhibited an induction period of 2 to 4 days. In the crystals of the rest of the compounds, dimerization initiated soon after exposure to UV light. The configuration of all the eight dimers was found to be syn head-head by ^{1}H-NMR spectra.

X-ray crystallographic analyses of 7-chloro, 7-methyl, 4-methyl-6-chloro, and 4-methyl-7-chloro coumarins were undertaken to correlate crystalline photoreactivity with molecular packing. The intensity data were collected on a Nonius CAD-4 diffractometer and the four structures were solved by direct methods (MULTAN-80). The crystal data for the four coumarins and the final R-factors are recorded below:

	7-chloro	4-methyl-7-chloro	7-methyl	4-methyl-6-chloro
a (Å)	4.454(1)	4 083(2)	13.130(1)	7 161(2)
b (Å)	30.488(6)	9 728(2)	18 600(1)	8.903(2)
c (Å)	5.684(2)	10 870(3)	6.587(1)	13.775(3)
α (°)	90	90	90	90
β (°)	91 21(2)	90 91(3)	90	104 04(2)
γ (°)	90	90	90	90
Z	4	2	8	4
Space group	$P2_1/n$	$P2_1$	pbca	$P2_1/c$
R	0.085	0.058	0 069	0 14

7-Chlorocoumarin and 4-methyl-7-chlorocoumarin possessed β-type of packing characterised by a short axis of 4.45 and 4.08 Å respectively. These two produced syn head-head dimers which were the direct consequence of their β-type structures The preliminary cell dimensions of 6-chlorocoumarins suggested that it possessed a short axis of 4.04 Å characteristic of a β-structure. It yielded the syn head-head dimer expected from β-packing. The crystal structure of 6-acetoxycoumarin, solved recently by Murthy *et al*[2], of our laboratory, revealed that the molecules are arranged in β-type of packing with a short axis of 3 90 Å. Syn head-head dimer produced is consistent with the above observation. Hence it is concluded that the photodimerization of 6-chloro, 7-chloro, 4-methyl-7-chloro and 6-acetoxycoumarins proceed *via* topochemical pathways. 4-Methyl-7-acetoxycoumarin produced syn head-head dimer the product expected from β-type structure. This behaviour is similar to that of 6-acetoxy and 7-acetoxy coumarins. The latter has been reported by Ramasubbu *et al*[3] to undergo topochemical dimerization to yield syn head-head dimer consistent with its β-packing Moreover, similar to the other coumarins discussed above, the reaction of 4-methyl-7-acetoxycoumarin also exhibited no induction period

The packing arrangements of 7-methyl and 4-methyl-6-chlorocoumarins suggested that the double bonds of these two compounds are well separated from each other (> 4.2 Å) *i.e.*, the packing arrangements were not conducive for a photoreaction. But they underwent photodimerization yielding syn head-head dimers. Moreover, these reactions involved substantial induction periods (2-4 days). These reactions were presumed to be non-topochemical. Similarly preliminary cell dimensions of 6-methoxycoumarin ($a = 6.73$, $b = 7.17$ and $c = 21.26$ Å) suggest that it does not possess β-packing although it yielded syn head-head dimer. It may, therefore, be concluded that the photodimerization of 6-methoxycoumarin is non-topochemical. It is noteworthy that the reaction of 6-methoxy-coumarin exhibited an induction period of 4 days as observed in 7-methyl and 4-methyl-6-chlorocoumarins

The usefulness of chloro and acetoxy substituents as steering agents in producing crystal structures conducive for photoreactivity is discussed. It has been found that the interchangeability of chloro and methyl groups based on their sizes[4] need not always be true. The present results obtained on photochemistry of coumarins allow us to gain an insight into the subtler aspects of topochemical postulates enunciated by Schmidt[5]. In the crystals of 7-chloro-coumarin the potentially reactive double bonds are separated by more than 4.2 Å (4.54 A) and it reacted to yield the topochemically expected syn head-head dimer It appears that a short distance ($< 4 2$ Å) between the reactive double bonds is not necessarily the only limiting factor for photodimerization in the solid state.

References

1 Bregman, J., Osaki, K., Schmidt, G. M. J and Sonntag, F. I	*J Chem Soc.*, 1964, 2021
2 Murthy, G. S, Ramamurthy, V. and Venkatesan, K	*Acta Cryst*, 1987, **C43** (in press).
3 Ramasubbu, N	*X-ray crystallographic investigation of strained small rings and some photoreactive coumarins*, Ph.D Thesis, Indian Institute of Science, Bangalore, 1982

4. Jones, W., Ramdas, S., Theocharis, C. R., Thomas, J. M. and Thomas, N. W	*J Phys Chem.*, 1981, **85**, 2594
5 Schmidt, G M. J.	*Pure Appl Chem.*, 1971, **27**, 647.

Thesis Abstract (Ph.D.)

Preparation and characterization of fuel cell electrodes by K. V. Ramesh.
Research supervisor: A. K. Shukla.
Department: Solid State and Structural Chemistry Unit.

1. Introduction

Fuel cells are one of the most effective devices for electrochemical energy conversion and storage in stationary as well as motive power applications[1]. Noble metals such as Pt, Pd, Ru and their alloys dispersed on porous carbon have been used as fuel cell electrodes in hydrogen-oxygen fuel cells[2]. These electrodes are rather expensive; however, their cost can be reduced by achieving maximum dispersion of the active metal or enhancing the catalytic activity by suitable pre-treatment of the electrodes. Although the activities of noble metal-supported carbon electrodes have been reported[3] to depend critically on chemical nature and composition of the catalyst, systematic characterization studies of noble catalyst is lacking in the literature. Such studies conducted in the present work reveal that systematic characterization of electrodes help in optimising catalyst loading and enhancing the activities of the electrodes. Catalytic activities of electrodes also depend on the type of carbon support employed. In the present work, a suitable method for obtaining active carbon from coconut shell charcoal has been developed.

2. Experimental

Active carbon was obtained from coconut shell charcoal by subjecting it to repeated soxhlet treatment with azeotropic HCl and gas activation under optimum conditions. Noble metals such as Pt, Pd, Ru and their alloys were impregnated on active carbon by different chemical methods. Electrodes were made by hot pressing catalyst-supported carbon mixed with polyethylene (binder) on platinum screens. Galvonostatic polarization and life-time studies for oxidation of hydrogen and ammonia and reduction of oxygen were conducted.

Catalysts were characterized by X-ray photoelectron spectroscopy (XPS), X-ray absorption spectroscopy (EXAFS), electron spin resonance (ESR), electron microscopy, X-ray and electron diffraction and BET surface area measurements.

3. Main results and discussion

The BET surface area of active carbon derived from coconut shell was 2000 m^2/g and had an ash content less than 0.05%. This carbon was found to be an effective support both for anodic oxidation of hydrogen and cathodic reduction of oxygen. The catalytic activities of electrodes were found to depend on particle size of carbon, chemical method of impregnating the catalyst on carbon, catalyst loading, binder composition, compaction pressure and working gas pressure.

Characterization of the platinum-supported carbon electrodes by XPS, EXAFS and ESR revealed the presence of oxides of platinum as impurity which retards its catalytic activity. On heat treatment in vacuum, the platinum on carbon was found to be free from oxides of platinum with mainly active platinum present. Hydrogen anodes prepared from vacuum heat-treated platinum on carbon exhibited maximum activity. These hydrogen anodes could sustain load currents up to 350 mA cm^{-2}, 800 mA cm^{-2} and 500 mA cm^{-2} for extended durations at 60°C in 6M KOH, 2.5 M H_2SO_4 and 7 M H_3PO_4 electrolytes respectively Studies with X-ray diffraction and electron microscopy, however, reveal that the vacuum heat treatment of the platinum-supported carbon causes sintering of the platinum crystallites resulting in a decrease in the available surface area of active platinum. It therefore becomes desirable to find an alternative chemical pathway wherein such losses in catalytic activity could be averted.

Platinum-group bimetals are known to exert a synergistic effect on the electro-catalysis of fuel cell reactions[4]. Galvonostatic polarization studies for hydrogen oxidation on carbon electrodes containing platinum group bimetal catalysts *viz.*, Pt-Ru, Pt-Pd and Pd-Ru showed that 4 wt% Pt + 6 wt% Ru on carbon electrodes exhibited maximum activity. This activity was higher than those of individual metal catalysts. XPS, EXAFS and ESR studies conducted on these electrodes reveals the presence of ruthenium which suppresses the formation of the oxidic impurities of platinum. In addition, electron micrographs of 4 wt% Pt + 6 wt% Ru on carbon showed higher dispersion and finer particles of the catalyst in relation to either platinum on carbon or vacuum heat-treated platinum on carbon. Furthermore, X-ray diffraction and electron diffraction studies demonstrated that the catalyst particles of Pt-Ru are amorphous unlike platinum-supported carbon electrodes wherein the platinum particles are found to be crystalline These electrodes could sustain load currents up to 500 mA cm^{-2}, 700 mA cm^{-2} and 800 mA cm^{-2} for extended durations in 6M KOH, 7M H_3PO_4 and 2.5M H_2SO_4 electrolytes respectively. This performance is superior to that of platinum-supported carbon electrodes. Typical polarization curve for a 4 wt% Pt + 6 wt% Ru/C electrode in 6M KOH shown at 60°C is shown in fig 1.

A wide variety of active carbons have been documented[5] as possible electrode substrates for oxygen-reducing electrodes in acid electrolytes. Electrochemical studies conducted to examine the feasibility of coconut-shell charcoal as support for oxygen-reducing electrodes showed it to be promising. The overall performance of platinum-supported carbon electrodes in acid electrolytes is comparable with the best type of platinized-carbon electrodes reported in the literature[6]

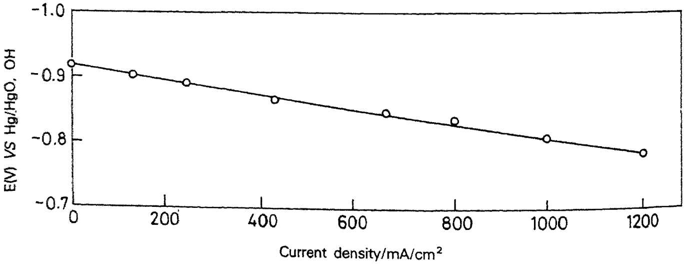

ɪɢ 1. Polarization curve (without IR correction) for hydrogen oxidation on a 4wt% Pt + 6wt% Ru/C lectrode in 6M KOH at 60°C.

Further, the performance of electrodes with bimetal catalysts *viz*, 4 wt% Pt + 6wt% Ru/C and 4 wt% Pt + 6wt% Pd/C was found to be superior to those with individual metal catalysts

Even for indirect ammonia oxidation, 4 wt% Pt + 6wt% Ru/C electrodes exhibited maximum activity (In indirect ammonia oxidation, ammonia is catalytically decomposed to nitrogen and hydrogen and the mixture is directly fed to the anode) It was also found that bimetal supported carbon electrodes oxidise ammonia more efficiently than the vacuum heat-treated platinum on carbon electrodes.

References

1 YEAGER, E	*Electrochemistry in industry New directions* edited by Uziel Landau, E. Yeager and D Kortan, Plenum Press, 1982, p 29
2. KINOSHITA, K AND STONEHART, P	*Modern aspects of electrochemistry* edited by J O'M Bockris and B. E Conway, Plenum Press, 1977, p 183.
3 BARD, A AND FAULKNER, L R	*Electrochemical methods, fundamentals and applications*, John Wiley, 1980, p 577
4 STONEHART, P.	*Adv Hydrogen Energy*, 1982, **3**, 1149
5 MANOHARAN, R	*Oxygen-reducing carbon electrodes for alkaline fuel-air fuel cells and metal-air batteries*, Ph D. Thesis, Indian Institute of Science, Bangalore, 1984
6 HOROWITZ, H. S LONGO, J. M. AND HOROWITZ, H H	*J. Electrochem Soc*, 1983, **130**, 1851–1859

Thesis Abstract (Ph.D.)

Studies on metal hydrazinecarboxylates: Precursors to fine particle oxide materials by P. Ravindranathan.

Research supervisor: K. C. Patil.
Department: Inorganic and Physical Chemistry.

1. Introduction

Fine particle oxide materials have a variety of applications Simple metal oxides find use as catalysts and are more reactive in solid-state reactions. Mixed oxide materials such as ferrites, cobaltites are used in the preparation of ferromagnetic liquids, high-density materials, catalysts, etc.

Preparation of fine particle oxides involves either breaking down or building up methods. Of the various methods reported in literature the solid solution precursor[1] technique is known to yield stoichiometric oxides on thermal decomposition. A variety of solid solutions of metal oxalates, carbonates, etc., have been used as precursors to mixed metal oxides. These anions when complexed with hydrazine are known to decompose at lower temperature to yield the oxides.

Although literature contains data on simple hydrazinecarboxylate derivatives[2], no data is available on mixed metal hydrazinecarboxylates and their possible use as precursors to the preparation of useful ceramic oxides. Thus it is aimed to prepare the simple and mixed metal hydrazinecarboxylates and examine the possibility of using them as precursors to fine particle oxide materials

2. Experimental

The instrumental methods used are simultaneous thermal analysis (Thermogravimetry-derivative thermogravimetry-differential thermal analysis, TG-DTG-DTA), differential scanning calorimetry (DSC), vibrating sample magnetometer (VSM), electrical conductivity measurements, particle size analysis (micron photosizer), surface area measurements, electron microscopy, X-ray powder diffraction, infrared and Mossbauer spectra

3. Results and conclusions

Metal hydrazinecarboxylates are usually prepared by the reaction of aqueous solutions of metal salts with hydrazine hydrate saturated with carbon dioxide The exact conditions to obtain a desired product have been standardised The following complexes have been prepared and characterized[3,4]

$M(N_2H_3COO)_2.nH_2O$ where M = Mg, Mn(n =2), Ca(n =1); $Ln(N_2H_3COO)_3.\ 3H_2O$ where Ln = Ce, Pr, Nd, Sm, Eu, Gd, Tb, Dy, Ho, Er, Yb and Y.

$M(N_2H_3COO)_2.\ (N_2H_4)_2$ where M = Mn, Fe, Co, Ni and Zn; and $N_2H_5M(N_2H_3COO)_3.\ H_2O$ where M = Mn, Fe, Co, Ni and Zn.

Infrared spectra of the complexes have been used to identify and differentiate e g the N-N stretching frequencies of $N_2H_3COO^-$, N_2H_4 and $N_2H_5^+$ occurring in the region 990-1005 cm^{-1} 925-930 cm^{-1} and 965 cm^{-1} respectively serve as finger prints to identify and distinguish between the hydrated, hydrazine and hydrazinium metal hydrazinecarboxylate derivatives.

Transition metal hydrazinecarboxylate derivatives, $M(N_2H_3COO)_2\ (N_2H_4)_2$ and $N_2H_5M(N_2H_3COO)_3.\ H_2O$ where M = Fe, Co, Ni and Zn decompose in a single step (in the temperature region 100–400°C) and exhibit autocatalytic combustion behaviour, accompanied by the evolution of large amounts of gases like NH_3, H_2O, N_2 and CO_2 to yield fine particle residues with large surface area (20–60 m^2/g).

Iron hydrazinecarboxylate derivatives, $Fe(N_2H_3COO)_2\ (N_2H_4)_2$ and $N_2H_5Fe\ (N_2H_3COO)_3\ H_2O$ decompose at 250°C to yield fine particle γ-Fe_2O_3 (used as recording material) and Fe_3O_4 in air and vacuum respectively[5].

The reactivity of fine particle oxide materials is demonstrated by the solid-state reaction between Zno and Fe_2O_3 at 900°C, 24 h to yield single phase $ZnFe_2O_4$.

Solid solutions of hydrazinium metal hydrazinecarboxylates $N_2H_5M_{1/3}\ Fe_{2/3}\ (N_2H_3COO)_3 \cdot H_2O$; M =Mg, Mn, Fe, Co, Ni and Zn have been prepared and investigated as precursors to ultrafine particle ferrites[6]. These complexes decompose autocatalytically at as low a temperature as 75°C to yield ultrafine ferrites. The decomposition has also been carried out in melt to minimise the size of the particles and to narrow down the size distribution. Mechanism for the formation of fine particles by the low-temperature autocatalytic gas-generating exothermic decomposition of the precursors has been discussed. Fine particle nature of the oxides is confirmed by XRD, TEM studies and particle size analysis. The ferrites obtained thus have large sruface area (100–140 m^2/g) and achieve 99% of theoretical density when sintered at low temperatures ($\leq$ 1000°C) than the normal sintering temperature ($\geq$ 1200°C). The particles are found to be superparamagnetic in nature at room temperature.

Technologically important fine particle Ni-Zn ferrites[7] have been prepared by the thermal decomposition/combustion of solid solution precursors; $N_2H_5(Ni_xZn_{1-x})Fe(N_2H_3COO)_3 \cdot H_2O$, where $x = 0.2–0.8$.

Preparation of fine particle mixed oxides by the thermal decomposition/combustion of solid solution precursors has been successfully extended to the preparation of fine particle cobaltites[8] using $N_2H_5M_{1/3}Co_{2/3}(N_2H_3COO)_3 \cdot H_2O$ M = Mg, Mn, Fe, Ni and Zn precursors. Nickel cobaltite obtained by this method has been tested for its electrochemical performance as an electrocatalyst in oxygen reduction reaction.

References

1 Longo, J. M Horowitz, H C. and Clavenna, L R	Solid state precursors. A low temperature route to complex oxides, in *Solid state chemistry: A contemporary overview* edited by S L. Holt, J. M Milstein and M Robbins. American Chemical Society, Washington, D C., 1980, 139–150
2 Schmidt, E. W	*Hydrazine and its derivatives*, John Wiley, 1984, 383–385.
3 Ravindranathan, P and Patil K C	Preparation, characterization and thermal analysis of metal hydrazinocarboxylate derivatives, *Proc Indian Acad. Sci., (Chem. Sci)*, 1985, **95**, 345–356
4. Mahesh, G. V Ravindranathan, P. and Patil, K. C	Preparation, characterization and thermal analysis of rare earth and uranyl hydrazinecarboxylate derivatives, *Proc. Indian Acad. Sci., (Chem. Sci.)*, 1986, **97**, 117–123
5. Ravindranathan, P and Patil, K C.	A one-step process for the preparation of γ-Fe_2O_3, *J Mater. Sci Lett.*, 1986, **5**, 221–222.
6 Ravindranathan, P and Patil, K C	A low temperature path to the preparation of ultrafine ferrites, *Am. Ceram. Soc Bull* 1987, **66**, 688–692
7 Ravindranathan, P and Patil, K C	Novel solid solution precursor method for the preparation of ultrafine Ni–Zn ferrites, *J Mater, Sci.* 1987, **22**, 3261–3264.
8. Ravindranathan, P Mahesh, G V and Patil, K. C	Low-temperature preparation of fine-particle cobaltites, *J Solid St. Chem.*, 1987, **66**, 20–25.

Thesis Abstract (Ph.D.)

Geology, geochemistry and mineralogy of mafic-ultramafic gneissic and cordierite gneiss enclaves of the Southeastern sector, Karnataka Craton, by K. S. Godhavari.
Research supervisor: G V. Anantha Iyer.
Department: Inorganic and Physical Chemistry.

1. Introduction

Four crustal components have been recognised in the eastern block of Karnataka Craton as in the western block. They are: 1. Cordierite-bearing gneisses (Sargur Group), 2. Migmatitic gneisses of Bangalore region, 3. Kolar green stone belt (Dharwar Supergroup) and 4. Patna and Closepet granites and homogeneous granites of Bangalore Geological, isotopic, geochemical and mineralogical studies carried out on those crustal components are summarised

2. Chronostratigraphy

The field observations supplemented with the published Rb/Sr whole-rock isochron age data[1-3] have been used to establish the relationship between the crustal components. The relationship between these crustal components leads to an understanding of the evolutionary history of the magmatite terrane of southeastern sector of the Karnataka Craton. The chrono-stratigraphic relation between the major crustal components is summarised below.

Age	$(87_{Sr}/86_{Sr})_i$	Lithological units
2600 Ma	0.7010 to 0.7032	Homogeneous granites of Bangalore
2650 Ma	0.7056	Patna and Closepet granites, Kolar Greenstone belt (Dharwar Supergroup)
2950 Ma	0.7057	Migmatitic gneisses of Bangalore
3010 Ma	0.7010	Cordierite-bearing Gneisses (Sargur Group)

This correlates with the lithostratigraphic relations provided for the Western Block[4].

The pre-metamorphic history of the enclaves of the cordierite gneiss, mafi-ultramafic rocks and migmatitic gneisses within the younger granitic rocks has been elucidated The Sr-isotope data suggests that the amphibolites, migmatitic gneisses and the cordierite-bearing rocks record a tectono-thermal metamorphic event around 3000 Ma. The peak metamorphic conditions are 5.2 kb and 710°C. This corresponds to a depth of about 25 km, indicating that the migmatite terrain presents a moderately deep section of the Archaean crust.

3. Petrogenesis

The petrogenesis of the major crustal components have been resolved with critical trends of chemical variation. The detailed geochemical investigation indicates that the cordierite-bearing gneisses are para in nature while the mafic-ultramafic enclaves are of igneous parentage. The migmatitic gneisses with high initial Sr-isotope ratios (0.7054) and REE abundance levels suggest that they are products of crustal anatexis. The granitic rocks from the migmatitie quarries of Bangalore with initial Sr-isotope ratios not exceeding 0.7035 and highly fractionated REE patterns suggest that they are derived from Archaean mantle source. On the other hand, the granitic rocks of Patna and Closepet with high REE abundance levels and high Sr-isotope ratio indicate that they are products of partial melting of Peninsular gneisses

4. Mineral chemistry

Mineral chemistry investigation of calcic amphiboles from mafic rocks, alkali feldspars from granitic rocks and cordierites from cordierite-bearing gneisses was undertaken to understand the conditions of their formation.

The calcic amphiboles investigated show a decrease in Si from 7.1 to 6.4 indicating the role of fluid pressure in their formation. Further the narrow range of Al(IV) + Na(M4) values and increasing Al(VI) – Na (M4) values displayed by the amphiboles indicate the role of pressure rather than temperature during their formation

The alkali feldspars encountered in the granitic rocks of Bangalore show textural evidence for the triclinisation of untwinned orthoclases X-ray analysis indicates the presence of both monoclinic and triclinic feldspars The alkali feldspar from the pegmatite phase of these intrusive granitic rocks is highly triclinic. The pegmatites being the end products of magmatic fractionation, rich in hydrothermal fluids, develop only microclines of high triclinicity as revealed by the investigation of Parsons[5] On the other hand, the textural and X-ray analysis of alkali feldspars from Patna and Closepet granites suggest that the K-feldspar in them is formed due to microclinisation of plagioclase

Detailed investigations of the cordierite minerals using chemical, optical, X-ray and IR techniques reveal that the distortion index values do not depend entirely on the composition alone The observed distortion indices in the cordierite grains do provide a measure for Al/Si order[6]

The study of channel constituents in the cordierites have been meaningfully used as fugacity indicators in rocks The present study reveals that one set of cordierite-bearing gneisses from the migmatite terrain are formed dominantly under f_{H_2O} conditions while the other set associated with charnockitic rocks are formed under dominant f_{CO_2} conditions similar to the contemporaneous formation of Closepet granite and charnockites as reported by Friend[7]

References

1 Beckinsale, R D, Reeve Smith, G, Gale, N H, Halt, R W and Thomson, B — Rb-Sr and Pb-Pb whole rock isochron ages and REE data for Archaean gneisses and granites, Karnataka State, South India, *Indo-U S Workshop on Precambrian of South India*, NGRI, Hyderabad (abstract) 1982, pp 35–36

2 Jayaram, S — *Geochemistry and geochronology of certain characteristic rock types of Dharwar Craton*, Ph D thesis, Indian Institute of Science, Bangalore, 1980

3 Venkatasubramanian, V S and Narayanaswamy, R — *Studies in Rb-Sr geochronology and trace element geochemistry in granitoids of Mysore Craton, J Indian Inst Sci*, 1974, **56**, 19–42.

4 Swaminath, J, and Ramakrishnan, M — Early precambrian supracrustals of Southern Karnataka, *Mem. 112. Geol, Surv India* 1981

5 Parsons, I — Feldspars and fluids in cooling plutons, *Mineral Mag*, 1978, **42**, 1–17

6 Putnis, A and Bish, D L — The mechanisms and kinetics of Al, Si ordering in Mg-cordierite, *Am. Mineral*, 1983, **68**, 60–65

7 Friend, C R L — Evidence for fluid pathways through Archaean crust and the Closepet granite, Karnataka, South India, *Precambrian Res*, 1985, **27**, 239–250.